Zeitschrift: Helvetica Physica Acta
Band: 47 (1974)
Heft: 3

Artikel: Charge transfer in transition metal alloys : a soft X-ray study
Autor: Wenger, A. / Steinemann, S.
DOI: https://doi.org/10.5169/seals-114574

Helvetica Physica Acta
Vol. 47, 1974 Birkhäuser Verlag Basel

Charge Transfer in Transition Metal Alloys— A Soft X-Ray Study

by **A. Wenger**[1]) and **S. Steinemann**
Institut de physique experimentale de l'Université de Lausanne

(25. IV. 74)

Abstract. A method is described for the direct determination of the changes on alloying of the number of $3d$ electrons on transition metal atoms. It is based on the measurement of ratios of relative integrated X-ray line intensities and on a phenomenological relation between the changes of $3d$ charge density inside the transition element ion and the change of the number of electrons in the d-band.

About fifty alloys of the binary systems of a transition metal (Ti, V, Cr, Mn, Fe, Co, Ni, Cu) with Al and Ni–Cu have been measured. Measurements concerning the $3p$ electrons of Al are also presented. In many cases, the results thus obtained can decide between two or more models for the electronic structure of these alloys as found in the literature. For Cu–Ni alloys no change for the number of d electrons on nickel atoms is found, in agreement with the minimum polarity model of Lang and Ehrenreich.

As is well known, bonding in metallic alloys may have partial ionic character, e.g. charge transfer between constituents accompanies compound formation. The notion of charge transfers is used in laws referring to the formation of classes of alloys and introduced in model electronic structures for the interpretation of various properties of specific alloys. This charge transfer is then understood as a global quantity, having a simple physical meaning. On the other hand, for band theories of alloys and compounds experimental charge transfer data are relevant for electron interactions or can simplify the choice of a potential.

Literature however reveals much controversy on the subject and in fact no simultaneously unambiguous and precise method exists for measuring charge transfers. A direct method is the Fourier synthesis of X-ray diffraction lines. Black and Taylor [1] applied it to transition metal aluminium alloys but could not obtain definite conclusions for the charge transfer; extinction corrections are uncertain and the overall precision for the electron densities is low. Indirect methods like X-ray line shifts, energy level shifts measured by 'electron spectroscopy for chemical analysis' (ESCA), Mössbauer isomer shift and magnetic measurements lack sure interpretation.

We present a new method for determining charge transfers which is based on the measurement of integrated intensities of X-ray lines and bands [2]. Like the diffraction method, it is direct in the sense that the measured quantity is directly sensitive to local charge densities. The method is applied to the system of binary alloys of the transition metals of the first series with aluminium and Cu–Ni [3].

---

[1]) Now at National Research Council of Canada, Ottawa.

1. Theory

1.1. X-ray emission intensity in pure metals and alloys

The specific example of an iron atom in an iron matrix or in an FeAl alloy is chosen (Fig. 1). Under an electron beam of sufficient energy, the Fe atom will be ionized $P_{(L_3)}$ times per second in the L_3 level (the $2p^{3/2}$ and $3s$ levels are also noted L_3

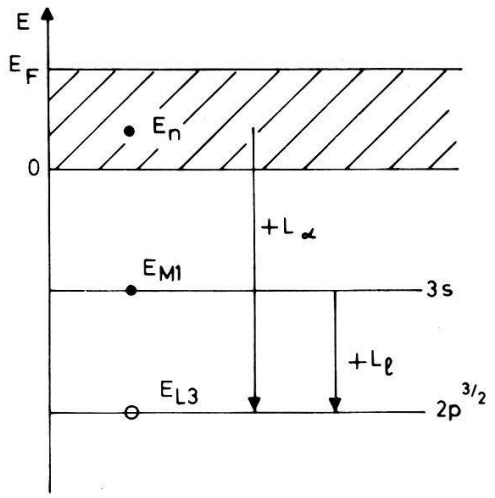

Figure 1
Transition scheme of soft X-ray emission in transition metals of the first series.

and M_1 respectively, and X-rays resulting from the transitions $(3d,\ 4s) \rightarrow 2p^{3/2}$, $3s \rightarrow 2p^{3/2}$ are called L_α and L_l). The probability per second for an electron with wave function $\psi_e(r)$ making a transition to this hole and emitting a photon is proportional to

$$P(e \rightarrow 2p^{3/2}) = \left| \int \psi_e(\vec{r})\, \vec{r} \psi^{*3/2}_{2p}(\vec{r})\, d\vec{r} \right|^2 \tag{1}$$

in the electric-dipole approximation [4]. P is different from zero only for $(3s \rightarrow 2p^{3/2})$ and $(n \rightarrow 2p^{3/2})$ transitions where n denotes a conduction electron. For the $(3s \rightarrow 2p^{3/2})$ transition (1) becomes

$$P(3s \rightarrow 2p^{3/2}) = 2F^2(R_{3s}, R^{3/2}_{2p}) \tag{2}$$

where $F(R_1, R_2) = \int_0^\infty R_1(r)\, r R_2(r)\, r^2\, dr$ and R_{3s}, $R^{3/2}_{2p}$ are the radial wave functions of the $3s$ and $2p^{3/2}$ states. Let $\psi_n(\vec{r})$ be the conduction electron wave function, which is a solution of $H\psi_n = E_n\psi_n$. H is the one-electron Hamiltonian for either the pure iron or alloy state: $H = (\hbar^2/2m)\Delta + V(r)$. If R_i be the radius of a sphere inside of which $V(\vec{r})$ is to a good approximation spherical (in APW calculations, R_i is in general the radius of the WS inscribed sphere), then for $r < R_i$, $\psi_n(\vec{r})$ may be expanded as

$$\sum_{l,m} A^n_{l,m} R^{E_n}_l(r)\, Y^m_l(\theta, \psi).$$

By a suitable choice of R_i, such that $R^{3/2}_{2p} \approx 0$ for $r > R_i$, formula (1) results in

$$P(n \rightarrow 2p^{3/2}) = F^2(R^{E_n}_{4s}, R^{3/2}_{2p})|A^n_{00}|^2 + \tfrac{2}{5}F^2(R^{E_n}_{3d}, R^{3/2}_{2p}) \cdot \left(\sum_{m=-2}^{+2} |A^n_{2,m}|^2 \right). \tag{3}$$

The number of emitted photons per second with energy between $h\nu$ and $h\nu + d(h\nu)$ is given by

$$I_{L_l}(h\nu)\, d(h\nu) = \frac{P_{(L_3)}}{P_{(tot)}} \cdot P(3s \to 2p^{3/2})\, \delta(E_{M_1} - E_{L_3} - h\nu)\, d(h\nu) \tag{4}$$

for the L_l line and by

$$I_{L_\alpha}(h\nu)\, d(h\nu) = \frac{P_{(L_3)}}{P_{(tot)}} \cdot \sum_n P(n \to 2p^{3/2})\, \delta(E_n - E_{L_3} - h\nu)\, d(h\nu) \tag{5}$$

for the L_α band. $P_{(tot)}$ is the probability per second for the $2p^{3/2}$ hole being filled. If, further, R_l^{En} is normalized by $\int_0^{R_i} R_l^{2En} r^2\, dr = 1$ then $\sum_m |A^n_{l,m}|^2$ is the charge of l symmetry inside the sphere of radius R_i contributed by the conduction electrons and $N_l(E) = \sum_{n,m} |A^n_{l,m}|^2 \delta(E - E_n)$ is the density of states of l symmetry inside this sphere. Thus (5) becomes

$$I_{L_\alpha}(E - E_{L_3}) = \frac{P_{(L_3)}}{P_{(tot)}} \{F^2(R^E_{4s}, R^{3/2}_{2p})\, N_s(E) + \tfrac{2}{5} F^2(R^E_{3d}, R^{3/2}_{2p})\, N_d(E)\}. \tag{6}$$

Equation (6) can in principle be used to test band structure calculations. However, it is only for light metals (Li, Be for K spectra, Na, Mg, Al . . . for L spectra) that the recorded and calculated spectra are more or less comparable in detail; for the L spectra of transition metals, the situation is less favourable (see e.g. Fig. 5 in Ref. [5]), the main reasons being that

a) the L_3 level has a considerable width $\delta \sim 1$ eV [6]. A distribution function $g(E)$ is often taken to be Lorentzian $g(E - E_{L_3}) = \delta/\pi[(E - E_{L_3})^2 + \delta^2]$;
b) the final hole in the conduction band has a finite lifetime τ and therefore a spread in energy of the order $\Delta E \sim \hbar/\tau$. This 'Auger broadening' [7] may reach several electron-volt at the bottom of the band [8]. Different authors describe it by a distribution $f(E,E') = \Delta(E)/\pi|(E' - E)^2 + \Delta^2(E)|$ whose half-width is given by $\Delta(E) = W[1 - (E - E_0)/(E_F - E_0)]$ where E_0 and E_F are the energies of the bottom of the band and of the Fermi level [5, 8, 9]. Moreover the change of the shape of the L band by alloying is often rather feeble [10], and its study leads to rather qualitative conclusions.

But *integrated X-ray spectras* can give important characteristic quantities of the electronic structure, less detailed than partial densities of states but not affected by the above broadening effects. In fact the L_α integrated intensity is given by the double convolution product of (6) with the broadening functions $g(E)$ and $f(E,E')$ and these are by definition normalized [$\int dE\, g(E)\, dE = 1$ and $\int dE f(E',E) = 1$] and therefore disappear from the expression giving the integrated intensity

$$I^{int}_{L_\alpha} = \int I_{L_\alpha}(E - E_{L_3})\, dE$$

$$= \frac{P_{(L_3)}}{P_{(tot)}} \int_0^{E_F} \{F^2(R^E_{4s}, R^{3/2}_{2p})\, N_s(E) + \tfrac{2}{5} F^2(R^E_{3d}, R^{3/2}_{2p})\, N_d(E)\}\, dE. \tag{7}$$

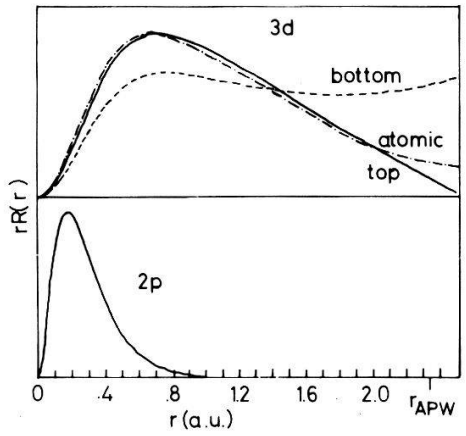

Figure 2
Radial wave functions for $2p$ electrons and atomic and metallic $3d$ electrons in iron following Wood [11] and Cuthill et al. [12].

Figure 2 shows the functions $rR_{3d}(r)$ for metallic and atomic iron and the function $rR_{2p}^{3/2}(r)$. Two facts appear:

a) For $r < r_i$ ($r_i \approx$ radius of the maximum of $rR_{3d}(r)$), the functions $rR_{3d}(r)$ for the top or the bottom of the iron band, or for atomic iron, are practically proportional one to another. This comes from the fact that in the radial equation which determines $rR_{3d}(r)$, and for sufficiently small values of r, the effective potential is very large compared to the changes of energy that occur when passing from one conduction electron to the other, from the pure metal to the alloy or from metallic iron to atomic iron (see Slater [13]).

b) Although $rR_{2p}^{3/2}$ is not yet quite negligible at values r, for which the various $3d$ wave functions begin to have different behaviour, we see in Figure 2 that $F(R_{3d}, R_{2p}^{3/2})$ will have very nearly the same value (at 10^{-3} relative accuracy) for the various $3d$ wave functions if these are made equal for small r values, this is realized by putting $R_i = r_i$ (about 0.7 a.u. for iron).

What has been stated for the $3d$ functions is even more pronounced for the $4s$ functions, because the effective potential is stronger, the $l(l+1)/r^2$ term being zero. Thus (by taking $R_i = r_i$) the F^2 are no longer a function of E and (7) can be directly integrated, giving

$$I_{L_\alpha}^{\text{int}} = \frac{P_{(L_3)}}{P_{(\text{tot})}} \{F^2(R_{4s}, R_{2p}^{3/2})\, n_s^i + \tfrac{2}{5} F^2(R_{3d}, R_{2p}^{3/2})\, n_d^i\}, \tag{8}$$

$n_l^i = \int_0^{E_F} N_l(E)\, dE$ being the charge of l symmetry deposited by the conduction electrons inside the sphere of radius r_i. In short n_s^i and n_d^i are the $4s$ and $3d$ charges inside the Fe ion.

In equation (8), the first term is small compared to the second one. Using the tables of Herman and Skillmann [14], the ratio $I_{L_\alpha}(3d)/I_{L_\alpha}(4s)$ of the intensities due to the $3d \to 2p^{3/2}$ and $4s \to 2p^{3/2}$ transitions for free atoms has been calculated. The result is given in Table I, together with values of the charge deposited by the $4s$ or the $3d$ electrons of the free atom in the sphere (of radius R_s) inscribed to the WS cell of the metallic element.

On the other hand, results of band structure calculations by Snow and Waber [15]

are referred to in Table II. The s, p, d columns give the charge of s, p, d symmetry in the sphere of radius R_s, whereas the 'ext' columns give the charge/atom outside this sphere. The calculations use two different potentials, built up from the charge distribution in a $s^1 d^{n-1}$ and $s^2 d^n$ configuration respectively.

Table I
Ratio $I_{L_\alpha}(3d)/I_{L_\alpha}(4s)$ of the intensities due to the $3d \rightarrow 2p^{3/2}$ and $4s \rightarrow 2p^{3/2}$ transitions, configuration and charge deposited in the WS cell by the $3d$ and $4s$ electrons

Element	V	Fe	Ni	Cu
R_s (a.u.)	2.483	2.436 (fcc) 2.345 (bcc)	2.354	2.415
Free atom electronic configuration	$3d^3\,4s^2$	$3d^6\,4s^2$	$3d^8\,4s^2$	$3d^{10}\,4s^1$
$\int_0^{R_s} r^2 R_{4s}^2(r)\,dr \times n_{4s}$	0.602			0.39
$\int_0^{R_s} r^2 R_{3d}^2(r)\,dr \times n_{3d}$	2.85			9.83
$I_{L_\alpha}(3d)/I_{L_\alpha}(4s)$	60	158	233	810

Table II
Band occupancy of l-like states calculated by Snow and Waber [15]

		Configuration $s^1\,d^{n+1}$				Configuration $s^2\,d^n$			
Element	n	s	p	d	ext.	s	p	d	ext.
Ti (bcc)	2	0.43	0.42	2.11	1.01	0.39	0.30	2.47	0.82
V (bcc)	3	0.40	0.42	3.07	1.08	0.37	0.33	3.36	0.92
Cr (bcc)	4	0.39	0.45	4.01	1.11	0.35	0.35	4.32	0.94
(fcc)	4	0.45	0.52	3.99	0.89	0.41	0.40	4.42	0.74
Mn (bcc)	5	0.43	0.43	5.14	0.96	0.35	0.26	5.67	0.69
(fcc)	5	0.47	0.53	5.13	0.82	0.40	0.32	5.64	0.60
Fe (bcc)	6	0.41	0.41	6.18	0.96	0.34	0.26	6.65	0.72
(fcc)	6	0.46	0.50	6.21	0.78	0.38	0.30	6.72	0.56
Co (fcc)	7	0.45	0.46	7.30	0.73	0.36	0.26	7.83	0.51
Ni (fcc)	8	0.44	0.39	8.48	0.64	0.32	0.21	9.02	0.42
Cu (fcc)	9	0.50	0.44	9.42	0.60	0.46	0.34	9.71	0.46

A comparison of these tables shows that the s and d charges inside the sphere of radius R_s are about equal in the metal and the free atom. Thus for the metal, as well as for the free atom, $I_{L_\alpha}(3d) \gg I_{L_\alpha}(4s)$, and therefore

$$I_{L_\alpha}^{\text{int}} = \frac{P_{(L_3)}}{P_{(\text{tot})}} \cdot \tfrac{2}{5} F^2(R_{3d}, R_{2p}^{3/2})\, n_d^l. \tag{9}$$

The integrated intensity of the L_l line is easily obtained from formula (4)

$$I_{L_l}^{\text{int}} = \frac{P_{(L_3)}}{P_{(\text{tot})}} \cdot 2F^2(R_{3s}, R_{2p}^{3/2}).$$

The ratio of the integrated intensity of the L_α band and the L_l line then is:

$$\frac{I^{\text{int}}_{L_\alpha}}{I^{\text{int}}_{L_l}} = \frac{1}{5}\frac{F^2(R_{3d}, R^{3/2}_{2p})}{F^2(R_{3s}, R^{3/2}_{2p})} \cdot n^i_d.$$

This ratio has interesting properties. The $R^{3/2}_{2p}$ and R_{3s} functions, being inner wave functions are only very weakly affected by chemical bonding, and the same is true for R_{3d} if it is normalized inside the sphere of radius r_i. F^2, appearing in the last equation, is thus the same in the pure metal and in the alloy and thus we define a ratio which characterizes this *charge transfer*:

$$R_L = \left.\frac{I^{\text{int}}_{L_\alpha}}{I^{\text{int}}_{L_l}}\right|_{\text{FeAl}} : \left.\frac{I^{\text{int}}_{L_\alpha}}{I^{\text{int}}_{L_l}}\right|_{\text{pure Fe}} = \frac{n^i_d(\text{FeAl})}{n^i_d(\text{Fe})} \tag{10}$$

or

$$R_L - 1 = \Delta n^i_d / n^i_d. \tag{10'}$$

Summarizing, we may say that measuring ratios of integrated X-ray intensities of the alloy and the pure metal gives the relative change of the number of $3d$ electrons inside the Fe ion when going from pure iron to the alloy (it must be noted that r_i must be exactly the same in Fe and FeAl, its exact value being less important).

1.2. Number of electrons in 'd-states' and relation to intensity ratios

In order to compare such spectroscopic results with other experiments or with models of electronic structure the above ratio R_L is to be related to the change of the number of $3d$ electrons. There is no unique and absolute definition in a solid for the number of electrons in d-states but different ones can be proposed:

a) $n^i_d = \text{constant} \cdot q^i_{3d} \cdot q^i_{3d}$ is the charge of d symmetry inside the Fe-ion. The constant is fixed for a given element. Formula (10') refers to this definition.
b) $n^{\text{APW}}_d = q^{\text{APW}}_{3d}$. This is the charge of d symmetry inside the APW sphere.
c) $n^{\text{WS}}_d = q^{\text{WS}}_{3d}$. This is the charge of d symmetry inside the WS sphere.
d) n_d = number of electrons in 'd-states', or in the 'd-band'. A transition metal atom has up to 10 d-states. This last definition is currently used in solid state physics, where a d-state is usually meant to be a solution of Schrödinger's equation with predominant but not exclusive d symmetry. Quoted values regarding definitions b), c) and d) differ by no more than 0.5 to 1 electrons in the pure metals and this is a consequence of the fact that $3d$ electrons are rather localized. For example, Table II gives $n^{\text{APW}}_d = 9.42$–9.71 for Cu and, as the external charge is only partially d-like, $9.5 \lesssim n^{\text{WS}}_d \lesssim 10$, whereas in the band picture one says that the d-band is full, i.e. $n_d = 10$. For Co, $n^{\text{APW}}_d = 7.3$–7.83 and $7.5 \lesssim n^{\text{WS}}_d \lesssim 8$ and, as the saturation moment of Co is $1.7\mu_B$, $n_d = 8.3$.

Definitions b) and c) are clearly applicable for pure metals only as there is no unique way of attributing an APW or WS sphere in alloys and compounds. Concerning definition d), a relation between the relative changes of n^i_d (which is what we measure) and of n_d is difficult to obtain by theory alone because no available band structure calculation of alloys give the wave functions required to calculate n^i_d. But an empirical

relation is possible. Amongst the alloys we have measured there are some for which the degree of filling of the d states in the pure metal and in the alloy is rather well known from other sources; this is the case for Cu and the Cu–Al system, for Ni, Ni_2Al_3 and $NiAl_3$, for Co and Co_2Al_9. Experimentation reported later show that, within experimental uncertainty,

$$R_L - 1 = \Delta n_d^i / n_d^i = \Delta n_d / n_d \tag{11}$$

whence

$$\Delta n_d = (R_L - 1) \cdot n_d \quad \text{(pure metal)}, \tag{11'}$$

which gives the change of the number of d electrons when going from the pure metal to the alloy. This relationship has been established experimentally for elements of the end of the transition series but is not necessarily quantitative for those of the first half. However, $\Delta n_d^i / n_d^i$ keeps the same precise meaning throughout the series.

For n_d (pure metal) of equation (11') the following values are used: Cu 10; Ni 9.5 (see Mott [16]); Co 8.3 (measurement of saturation magnetization); Fe 7 (magnetic measurements [17]; Compton profile measurements [18]). As already noted, these values are about $0.5e^-$ larger than the n_d^{APW} values of Snow and Waber. We shall therefore take for Mn, Cr, V and Ti the values n_d^{APW} of Snow and Waber augmented by about 0.5 electrons, that is 6, 5, 4 and 3 respectively. For V and Ti, the numbers thus obtained is in agreement with the value estimated from Compton profile measurements [19, 20].

1.3. *Intensities of the $K_{\beta x}$ band and K_α line of aluminium*

An equation similar to (10) is obtained for the K_α ($2p \rightarrow 1s$) line and K_β ($3p \rightarrow 1s$) band of aluminium. The measurement of integrated intensity ratios again gives information about the relative change of the number of p symmetry conduction electrons inside the Al ion upon alloying. For $r > 1$ a.u. (0.53 Å), $rR_{1s}(r)$ is vanishingly small [14], whereas for $r \lesssim 1$ Å, the shape of $rR_{3p}(r)$ is the same in pure Al, in the alloy, or in the free atom [2]. It is defined:

$$R_K = \frac{I_{K_{\beta x}}^{int}}{I_{K_\alpha}^{int}}\bigg|_{AlFe} : \frac{I_{K_\beta}^{int}}{I_{K_\alpha}^{int}}\bigg|_{pure\ Al} = \frac{n_p^i\,(AlFe)}{n_p^i\,(Al)} \tag{12}$$

or

$$R_K - 1 = \Delta n_p^i / n_p^i. \tag{12'}$$

Unlike the situation for d electrons, there is not, even approximately, a p band in the metals and alloys, but only a s–p band. To get an idea of the charge transfer involved, one can make the assumption that $\Delta n_p^i / n_p^i$ is equal to $\Delta n_p / n_p$ and put $n_p = 1$ for pure Al (n_p is the number of electrons of p symmetry inside the WS sphere).

1.4. *Remarks concerning the validity of the intensity ratio formulas*

Equations (10') and (12') derive from one-electron theory and neglect at least two effects, namely the influence of the transition metal $2p^{3/2}$ or Al $1s$ hole on the local electronic structure, and the presence of satellites on the high-energy side of the L_α emission.

The influence of the hole is in fact a complicated, time-dependent many-body problem, resulting from the interaction of the $2p$ (or $1s$) hole, the X-photon, the final hole in the conduction band and the conduction electrons. We are deficient of a theory which allows a numerical estimation of this effect, especially in the case of transition metals. A simple experimental procedure allows the suppression of high-energy satellites that is to work below the excitation voltage of the L_2 level [21]. The only known TM spectra recorded under this condition are those of pure Ni and Cu, obtained by Liefeld [21]. The intensities are about 100–1000 times weaker at these voltages than those of the present study and the conditions on the cleanness of the surface are drastic [22]; we have not been able to work at such low voltages and have had to include some of this satellite emission in the integrated intensities.

An estimate of the influence of these two effects on the validity of equations (10′) and (12′) cannot be made. It may be noted, however, that they will affect these results only as far as they are different in the pure metal and in the alloy. Moreover, the correlation obtained experimentally between R_L and Δn_d in Cu, Ni and Co alloys show that the one-electron theory may not be too far from the truth, at least as far as integrated intensities are concerned.

1.5. Comparison with other methods and similar studies

The X-ray line shift method has been applied with some success to chemical compounds, for which the shifts are often important [23, 24]. Applied to alloys it has given no quantitative result, mainly because of the difficulty of measuring these shifts (a maximum of a few tenths of an electron-volt for 5–10 keV lines, whose width is of the order of 1 eV) with sufficient accuracy. Thus a recent paper [25], where $K_{\alpha 12}$ displacements are given for some of the alloys of interest here, quotes $\Delta E = 0.1$ eV $\pm$ 0.1 eV for Ni_2Al_3, $\Delta E = 0.2$ eV $\pm$ 0.1 eV for NiAl and $\Delta E = 0.17$ eV $\pm$ 0.05 eV for FeAl. There are also considerable uncertainties when going from the shifts to the charge transfers [23].

ESCA allows an absolute measurement of the inner level shifts. Simple correlations have been established between calculated charge transfers and level shifts for various series of compounds [26]. However, in cases where electronic structure calculations are uncertain a quantitative deduction of charge transfers from these shifts is not yet possible.

The Mössbauer isomer shift is proportional to the total electronic density at the nucleus. Here, too, experimental results may be ambiguous (for example, this density increases either because there are more $4s$ electrons or because there are less $3d$ electrons [27]).

The most important information for this study comes from magnetic moment and susceptibility measurements. It is possible to deduce n_d from the magnetic moment only if the spin-up band is full and this is generally recognized to be the case for Ni and Co, but not for Fe. Deduced magnetic moments are 0.6 and 1.7 μ_B/at for Ni and Co, and from the gyromagnetic ratio of Ni, $g_{Ni} = 2.193$, one then gets $n_d = 9.45$ and 8.3 for pure Ni and Co.

There is no magnetic moment in Ni_2Al_3, $NiAl_3$ and Co_2Al_9, and these compounds have small ($\sim 10^{-5}$ cm^3/mole) and almost temperature-independent susceptibilities, what has been generally interpreted as resulting from a filled d shell [28–30]. However, it is certainly hazardous to draw the same conclusions for $MnAl_6$ and $CrAl_7$, as did Foex and Wucher [28], and Köster et al. [31]; a small temperature-independent

susceptibility only implies the absence of localized moments and a small density of states at the Fermi level, but not necessarily a filled $3d$ shell. Similarly, the fact that the susceptibility follows a Curie–Weiss law in a given range of temperature implies not necessarily that Hund's rule ($S = \frac{1}{2}n_d$ if $n_d \leqslant 5$, $S = 5 - \frac{1}{2}n_d$ if $n_d > 5$) applies, nor that the Curie constant has its simple meaning $C = N^2 n_{\text{eff}}^2/3R$ (N is Avogadro's number, R the gas constant and $n_{\text{eff}} = 2\sqrt{S(S+1)}$). Nevertheless, these are the assumptions made by Köster et al. [31] and Kopp and Wachtel [32] to estimate n_d in the Mn–Al and Cr–Al alloys.

Following the work of Shubaev [2] on chemical compounds, several Russian authors measured the relative integrated intensities $I_{K_{\beta 5}}/I_{K_{\beta 1}}$ of transition metal elements in alloys [33, 34]. The number of $4p$ electrons is small (0.2–0.5) and the weak $K_{\beta 5}$ band lies on the high-energy tail of the intense $K_{\beta 1}$ line. This makes any figure of a charge transfer uncertain.

Spectroscopic measurements involving d electrons of transition metals have been made by Lukirskii and Brytov on Ti and Cr oxides [35]. Their results for integrated intensities are, however, strongly affected by reabsorption effects.

2. Experimental Procedures

We give here only an account of the techniques used and interested readers may consult Ref. [36] for details. The measurements were made on an ARL microprobe (EMX). The sample surfaces were prepared by standard metallographic techniques and the natural oxide layer was removed by ionic attack inside the microprobe. With normal vacuum conditions (about $5 \cdot 10^{-6}$ torr) the oxide layer thickness increases under the electron beam. This effect was reduced by making a scanning of the electron probe, which thus remained only 10–15 seconds on each point of the surface. The thickness of the oxide layer was controlled before and after each measurement by monitoring the oxygen K_α line intensity. The carbon contamination was suppressed by a liquid nitrogen trap.

The integrated intensities were measured directly by scanning the wavelength linearly in time and accumulating the counts.

The measured ratios of integrated intensities have to be corrected for reabsorption. For the emission bands, the absorption coefficient μ/ρ varies across the band. However, for the rather low acceleration voltages, the absorption coefficient was taken as an average $\overline{\mu/\rho} = \int I(\lambda)\mu/\rho(\lambda)\,d\lambda / \int I(\lambda)\,d\lambda$. The values of μ/ρ were taken from various published absorption coefficient tables and curves. It must be noted that if aluminium is alloyed to a transition metal, the absorption curve of the latter may be modified. This will be particularly important if the d shell is full in the alloy, and not in the pure metal. As will be seen later this seems to be the case for NiAl, Ni_2Al_3, Co_2Al_5 and Co_2Al_9. For these alloys the absorption curves of Bonnelle [6] were used, in which the so-called white line was truncated (Ref. [37] gives an example of such a variation). In all other cases, the same absorption, $\overline{\mu/\rho}$, was used for the pure metal and the alloy.

The acceleration voltage was chosen so as to make the errors on R, due to the uncertainty of the absorption correction and to the residual oxide layer, both less than about 1%. In Table III are reported, for each binary system, the accelerating voltage, the maximum depth of X-ray excitation in the pure metal and in the most dilute alloy and the absorption correction factor for this alloy ($R = R_{\text{meas}} \cdot k$).

The integrated intensity of the L_α band $\{3d(4s) \rightarrow 2p^{3/2}\}$ corresponds, in Figure 3, to the surface enclosed by curve $ASGFEA$, whereas the measured curve is $ASGBS_1 \ldots$.

Table III
Accelerating voltage V, maximum depth of X-ray production Z_m and absorption factor k for the measurements

	V in kV	Z_m (pure) in Å	Z_m (alloy) in Å	k
Cu–$CuAl_2$	1.7	118	229	1.001
Ni–$NiAl_3$	1.6	109	240	1.018
Co–Co_2Al_9	1.5	101	241	1.02
Fe–$FeAl_3$	1.4	105	210	1.016
Mn–$MnAl_6$	1.6	160	346	1.033
Cr–$CrAl_7$	1.6	167	359	1.019
V–V_4Al_{41}	1.6	207	407	1.022
Ti–$TiAl_3$	1.6	279	390	1.042
Ni–$Ni_{20}Cu_{80}$	1.6	109	109.4	1.02

It is difficult to separate exactly the L_α and L_β $\{3d(4s) \rightarrow 2p^{1/2}\}$ bands, but as only the ratio of these integrated intensities in the pure metal and in the alloy is of interest, this is not very important. The surface $ASGBA$ is taken as integrated intensity, where B is at the minimum of curve L_α, L_β. This choice has the advantage of being insensitive to a small displacement of the L_α band when going from the pure metal to the alloy. Moreover, it reduces the importance of the high-energy satellite emission. One could also take the area enclosed by curve $ASGBCA$, supposing the area of 'triangles' DCF and CFE equal. These two methods (I and II) give values of R_L differing by less than 2–3% (0% for $CuAl_2$, –1% for $NiAl_3$, –2% for Co_2Al_9, –3% for $MnAl_6$, 0% for $CrAl_7$), the largest difference occurring for the Al-rich alloys. Moreover,

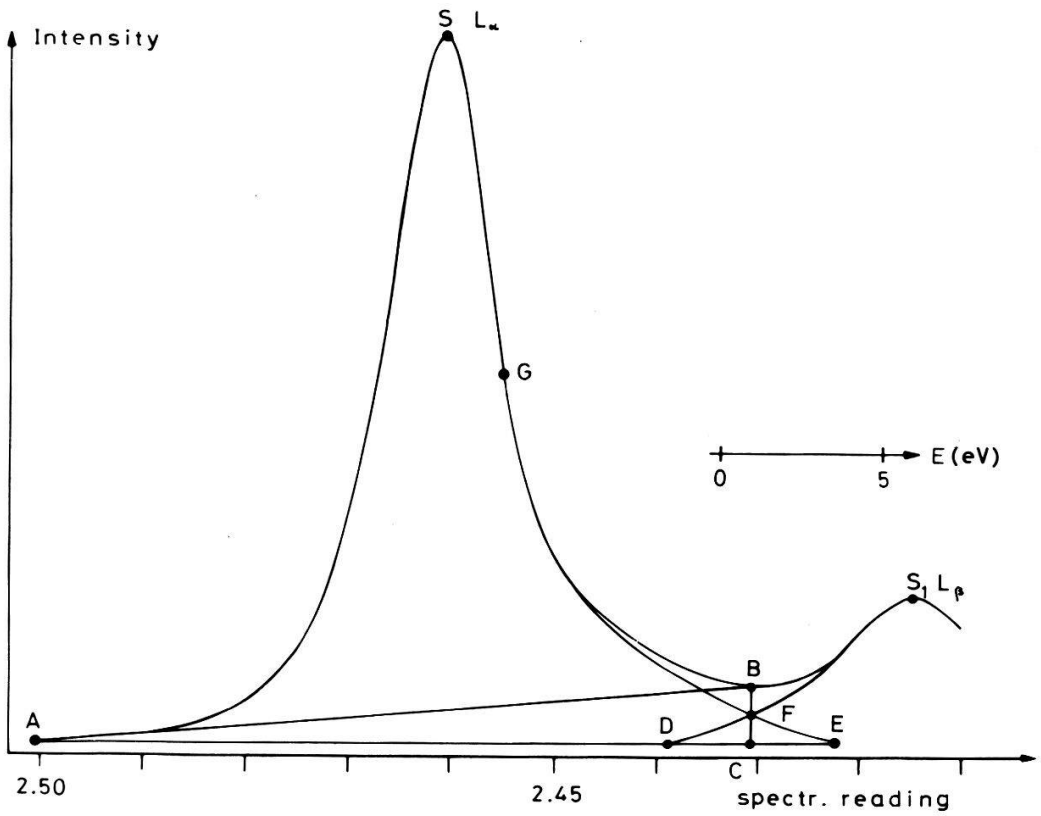

Figure 3
L_α and L_β emission spectrum of cobalt. The area $ASGBA$ is taken as integrated intensity (see text).

for Cr–Al the values of R obtained by integrating $L_\alpha + L_\beta$ gives, within experimental uncertainty, the same results as methods I and II (no data can be given to make the same comparison on other alloys). For Ti–Al, it is not possible to separate adequately the L_α and L_β bands, so R was calculated with the L_α and L_β integrated intensities. On the other hand, for the L_l ($3s \rightarrow 2p^{3/2}$) line, which partially overlaps the L_n ($3s \rightarrow 2p^{1/2}$) line we have used method I except for Ti–Al; in this case the overlap is too important and we have integrated the $L_l + L_n$ lines.

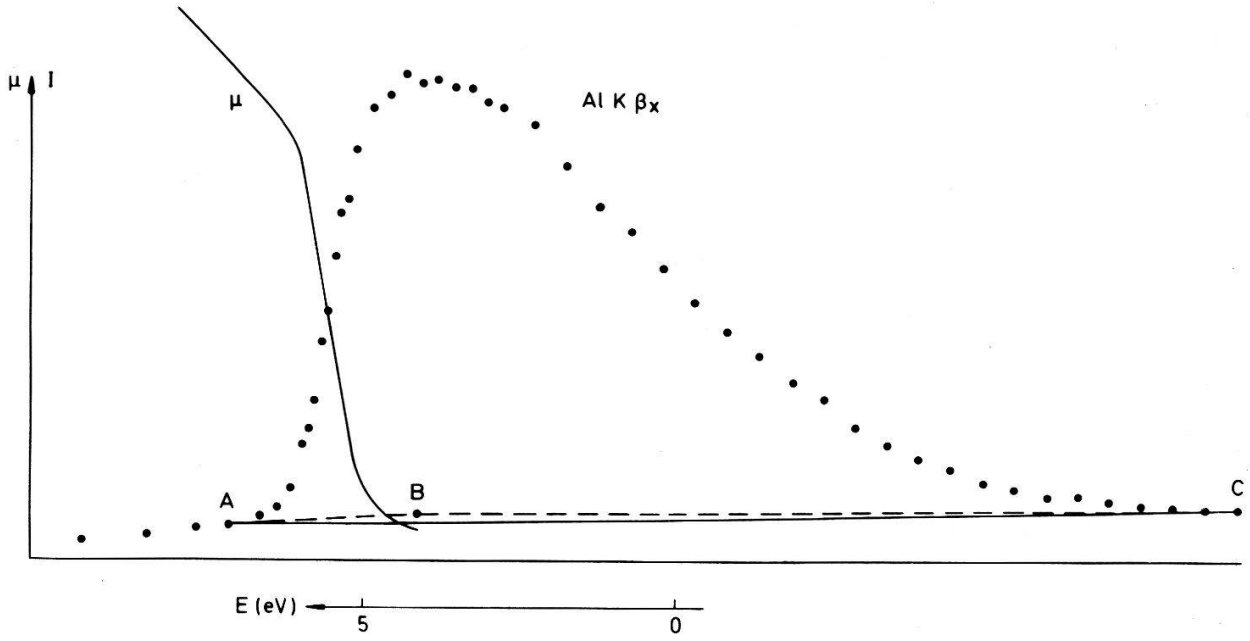

Figure 4
$K_{\beta x}$ emission and absorption spectrum of aluminium. Integration procedure explained in text.

Turning now to the integration of the K spectrum of aluminium, Figure 4 gives the $AlK_{\beta x}$ ($3p \rightarrow 1s$) emission band recorded in this study together with the absorption spectrum measured by Rudström [38]. There is some overlap between the two curves, as shown by the measurements of Nemnonov et al. [39]; this overlap becomes weaker when a transition metal is alloyed to aluminium. The straight line AC is taken as background, whereas the true background is ABC. The integrated intensity of $AlK_{\beta x}$ in pure Al is thus overestimated by 1–2% and less in the alloys, so R is slightly too small. The value on the long wavelength side of the K discontinuity is taken for μ/ρ (342 cm^2/g), whereas a graphical integration shows that its average $\overline{\mu/\rho}$ is 1.5 times larger. For the alloys the difference is less important, the overlap being smaller. By the procedure R is overestimated by at most 1%. Two errors of opposite sign are thus introduced, both of which are small (1–2%). As the absorption curves are known [39] only for Al-rich alloys, for which the absorption correction is in any case small, we found it better to correct for neither of these two errors.

Finally we say a few words about the alloys measured in this study. For the eight binary transition metal–aluminium and the Cu–Ni system 51 alloys were prepared. Compositions were chosen in the solid solution range and in regions of intermediate phases (the compositions appear in Figs. 5, 6 and 12). The purity of the starting materials were: 99.9–99.99% for Cu, Ni, Co, Fe, Mn, Cr; 99.6% for V and Ti; 99.99% for Al and 99.999% for Cu and Ni of the Cu–Ni alloys. Several techniques were used to make the alloys: a) melting in Al_2O_3 or MgO crucibles, casting and annealing;

b) solidification in a temperature gradient; c) melting in an electron beam furnace. The composition and homogeneity of the alloys were checked before and after annealing by metallographic examination and by microprobe analysis. For the specimens which were finally used for the measurements, the inhomogeneity $\Delta = \overline{|c - \bar{c}|}$ was never larger than 1–2% (c is the local atomic concentration of the alloy).

3. Results and Discussion: Transition Metal–Aluminium Alloys

3.1. A review of charge transfer data in the systems

The alloys have been extensively studied, both experimentally and theoretically. Raynor [40] tried to explain the phase diagram by assuming that the Al-rich alloys were 'electron compounds'. As a consequence the 3*d* shell is filled up in the Al-rich compounds $CrAl_7$, $MnAl_6$, $FeAl_3$, Co_2Al_9, $NiAl_3$, which implies an important electron transfer from the Al atom to the transition metal atom (4.66, 3.66, 2.66, 1.71, 0.61e^- for Cr, Mn, Fe, Co and Ni). In contradiction with this Pauling [41] published a model for the electronic structure of Co_2Al_9 in which charge transfer takes place in the opposite direction. Foex and Wucher [28] measured a weak temperature-independent para- or diamagnetism for the compounds $CrAl_7$, $MnAl_6$, $CoAl_4$, Co_4Al_{13}, Co_2Al_5 and $NiAl_3$, which they interpreted as resulting from a complete filling up of the 3*d* shell, in agreement with Raynor's theory. For $FeAl_3$ they found a Curie–Weiss law, showing that the 3*d* shell was not full in that case.

Meanwhile, in a review article, Hume-Rothery and Coles [17] expressed scepticism as regards Raynor's theory and considered as very unlikely to have ten *d* electrons on Cr, Mn or Fe atoms.

During the last ten years a great deal of magnetic and electrical measurements (Hall effect, resistivity) on these alloys were published. Taylor [42] made a systematic study of the susceptibility of the Al-rich alloys, which he divided into two groups: compounds of a first group comprising VAl_{10}, V_7Al_{45}, V_4Al_{23}, VAl_3, V_5Al_8, $CrAl_7$, Cr_2Al_{11}, $CrAl_4$, $MnAl_6$, Co_2Al_9, Co_4Al_{13}, $NiAl_3$ and Ni_2Al_3, which show a small ($0.1–1.5 \cdot 10^{-6}$ emu/g), almost temperature-independent paramagnetism, and others of a second group, namely $MnAl_4$, Mn_3Al_{10}, Mn_4Al_{11}, $FeAl_3$, $FeAl_2$ and Fe_2Al_5 having a high Curie–Weiss susceptibility. Taylor concluded that Raynor's 'absorption hypothesis' did not explain the magnetic behaviour of the Al–Fe, Al–Mn, Al–Cr system. However, Raynor postulated a full 3*d* shell only for the Al-richest compounds, so Taylor's measurements contradicts Raynor's hypothesis only for $FeAl_3$. Köster

Table IV
Number of 3*d*-electrons per transition metal atom as deduced from susceptibility measurements [30, 31]

	e^- 3*d*/at.		e^- 3*d*/at.
$MnAl_6$	10	$CrAl_7$	10
$MnAl_4$	9	Cr_2Al_{11}	9
$MnAl_3$	8	$CrAl_4$	8
Mn_5Al_8	7.5	Cr_4Al_9	7.5
Mn_6Al_7	7	Cr_5Al_8	6.6
δ-Mn	6.3	Cr_2Al	5.4
		Cr	5.4

et al. [31] and Kopp and Wachtel [32] also made susceptibility measurements on some of these alloys. For the Mn–Al and Cr–Al system, they find the number of $3d$ electrons per transition metal atom (in agreement with Raynor's theory) given in Table IV. Also from susceptibility measurements, Höhl [30, 43] found 0.01 and 0.62 hole per TM atom in $Ni_{50}Al_{50}$ and $Co_{50}Al_{50}$, whereas Butler et al. [44], from magnetic and electrical measurements, gave a model with 2 and 3 holes per transition metal atom.

3.2. *Measurements on the test alloys*

In the Cu–Al system, the d shell remains full for all concentrations. This shell is also likely to be full in the alloys Ni_2Al_3, $NiAl_3$, Co_2Al_9 (see Section 1.5). For all these alloys, called test alloys, it is thus possible to calculate the relative change $\Delta n_d/n_d$ of

Table V
Comparison between $R_L - 1$ and $\Delta n_d/n_d$ for the test alloys

Alloy	$R_L - 1 = \frac{\Delta n_d^i}{n_d^i}$ in % measured	$\frac{\Delta n_d}{n_d}$ in % calculated
$Cu_{80}Al_{20}$	-1 ± 0.7	0
CuAl	-0.6 ± 0.7	0
$CuAl_2$	-1 ± 0.8	0
Ni_2Al_3	5.1 ± 0.8	5.2 – 5.8
$NiAl_3$	5.0 ± 0.9	5.2 – 5.8
Co_2Al_9	19.3 ± 1.4	20.5

the number of electrons in d states when going from the pure metal to the alloy (n_d for the pure metal is known, see Section 1.2). On the other hand we have measured R_L. Table V shows that within experimental uncertainty $\Delta n_d/n_d$ is equal to $R_L - 1$; this allows us to formulate equation (11), i.e. the spectroscopically determined charge represents also band states in the alloy.

3.3. *Change of the number of d electrons for alloys of Al with metals at the end of the transition series*

Figure 5 gives the values of Δn_d deduced from the measured values of R_L by using equation (11'). The above results on the test alloys (Cu–Al: $\Delta n_d = 0 \pm 0.1$; Ni_2Al_3, $NiAl_3$: $\Delta n_d = 0.48 \pm 0.09$; Co_2Al_9: $\Delta n_d = 1.6 \pm 0.1$) correspond well with the expected values of $\Delta n_d = 0$ for Cu-alloys, $\Delta n_d = 10 - 9.45 = 0.55$ for Ni-alloys and $\Delta n_d = 10 - 8.3 = 1.7$ for Co_2Al_9.

For $Ni_{50}Al_{50}$, Höhl [30] (magnetic measurements) finds 0.01 hole in the d band, West [45] explains his NMR result with a full $3d$ band, while Butler et al. [44] interpret their magnetic and electrical measurements with a model in which there are two $3d$ holes. We find an almost filled $3d$ band (≈ 0.05 hole). From susceptibility measurements, de Boer et al. [46] found 0.35–0.42 $3d$ holes in Ni_3Al, in good agreement with our value (0.35). The susceptibility measurements on Co_2Al_5 [29] may also be interpreted with a filled $3d$ shell; however, we obtain the smaller value $\Delta n_d = 1.45 \pm 0.1$. For $Co_{50}Al_{50}$ one finds again very different values in the literature. Taking n_d (Co) = 8.3, Höhl [30] obtains $\Delta n_d = 1.08$ from susceptibility measurements, Raynor [40], assuming

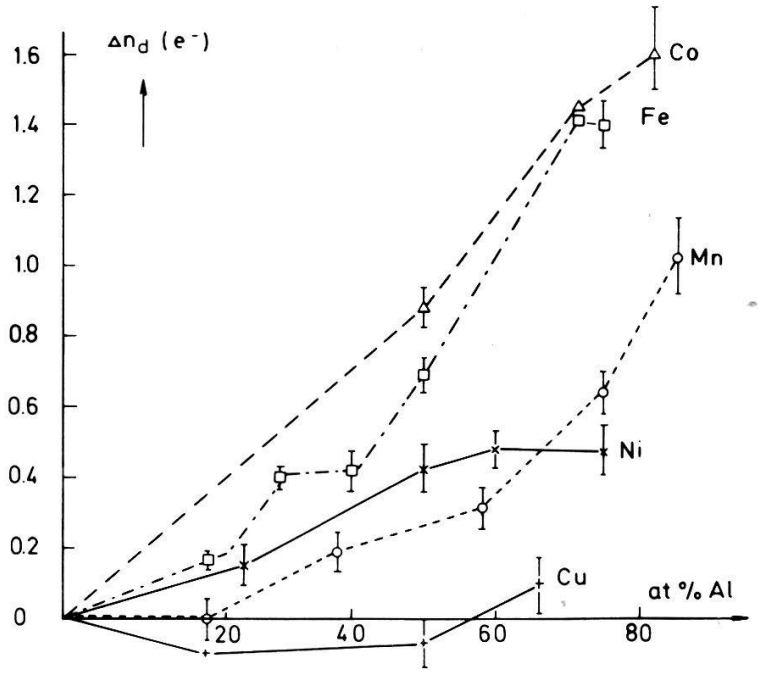

Figure 5
Measured charge transfers in Cu–Al, Ni–Al, Co–Al, Fe–Al and Mn–Al systems; the test alloys are Cu–Al, Ni_2Al_3, $NiAl_3$, Co_2Al_9.

that CoAl is an electron compound with $1.5e^-$/at. gets $\Delta n_d = 0.7$, while Butler et al. [44] obtain $\Delta n_d = -1.3$, in total disagreement with our value $\Delta n_d = 0.88 \pm 0.06$.

3.4. Change of the number of d electrons in the alloys Fe–Al and Mn–Al

$FeAl_3$ and Fe_2Al_5 follow a Curie–Weiss law from which Taylor [42] deduced a number of unpaired spins equal to 1.58 and 1.66. If Hund's rule applies, this leads to about 8.4 *d* electrons and, as Fe has about 7 *d* electrons (Section 1.2), one gets $\Delta n_d = 1.4$, which is exactly what we obtain for these alloys: $\Delta n_d = 1.4 \pm 0.07$ (Fig. 5).

Höhl [30] explains the temperature dependence of the susceptibility of $Fe_{50}Al_{50}$ and $Fe_{60}Al_{40}$ by a reduction of n_d with increasing temperature; thus at 300°K, he finds $\Delta n_d = 2$ and 0.6 for FeAl and $Fe_{60}Al_{40}$, in disagreement with our values $\Delta n_d = 0.69 \pm 0.05$ and 0.41 ± 0.06 respectively.

For iron-rich Fe–Al alloys, Edwards [47] proposed a model (Hubbard splitting) in which the itinerant *d* band just becomes full for $Fe_{70}Al_{30}$, leading to $\Delta n_d = 0.9$ for this alloy, whereas we find $\Delta n_d = 0.4 \pm 0.03$. Finally for $Fe_{80}Al_{20}$, Srinivasan and Claus [48] concluded from specific heat data of ternary alloys that n_d should be about 0.1 less in the alloy than in pure Fe. Our measured value of $\Delta n_d = +0.16 \pm 0.03$ contradicts this.

In the Mn–Al system, Δn_d is still positive, but for the Al-richest compound $MnAl_6$, our value $\Delta n_d = 1.2 \pm 0.12$ is much smaller than that predicted by Raynor's theory (full $3d$ shell $\Delta n_d = 4$) and that deduced by Köster et al. [31] from susceptibility measurements. These same authors find $\Delta n_d = 2$ and 1.5 for $MnAl_3$ and Mn_5Al_8, whereas we find 0.64 ± 0.06 and 0.32 ± 0.06 (Fig. 5).

3.5. Change of the number of d electrons in the alloy series Cr–Al, V–Al and Ti–Al

Figure 6 gives Δn_d calculated by equation (11′) from the measured values of R_L, taking $n_d = 5$, 4 and 3 for pure Cr, V and Ti respectively (see Sections 1, 2). For the

Cr–Al system, our values ($\Delta n_d \approx$ const. $= -0.35$) are in full disagreement with those deduced by Köster et al. [31] from susceptibility measurements, which give $\Delta n_d = 0$, +1.2, +2.1, +2.6, +3.6, +4.6 for Cr_2Al, Cr_5Al_8, Cr_4Al_9, $CrAl_4$, Cr_2Al_{11} and $CrAl_7$ respectively (these values for the last compound would agree with Raynor's theory).

The V–Al system is the only case where we found a non-monatomic change of Δn_d with concentration. The Al-rich phases VAl_{10}, V_4Al_{23} and VAl_7 have in fact some

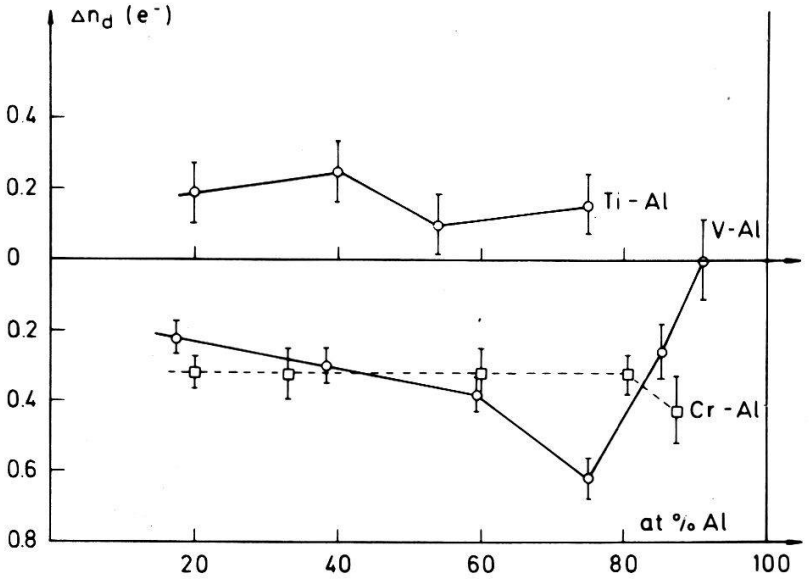

Figure 6
Measured charge transfers in Cr–Al, V–Al and Ti–Al systems.

particular properties; they have similar crystalline structures which are quite different from that of VAl_3 [49], their stability range is limited to about 700°C and their electronic specific heat coefficients are markedly high [50]. Thus, Δn_d shifts abruptly where other physical properties change suddenly. Ray and Smith [51] tried to get evidence of charge transfer in V_4Al_{23} by X-ray diffraction but they reached only the (rather qualitative) conclusion that an important charge transfer ($2e^-$ or more) is very unlikely in this compound and this confirms the present spectroscopic data.

Finally, in the Ti–Al system, Δn_d is positive again, but small. It may be concluded from this that the local electronic structure of Ti is rather slightly modified by the presence of Al atoms; one should remember that Al has anomalously large solubility in Ti.

3.6. Change of Δn_d with the element alloyed to aluminium

In Figure 7, Δn_d is plotted for fixed Al concentrations versus the alloyed transition metal. The following points appear:

a) Although these alloys have very different crystal structures and physical properties, the change of Δn_d with the alloyed element is rather regular and systematic; Δn_d is about zero at the beginning, the middle and the end of the transition metal series and is negative in the first half, positive in the second.

b) Raynor's theory [40], which predicts a complete filling of the *d* shell for the Al-richest alloys, is correct only at the end of the series.

c) Hume-Rothery and Coles [17] have analysed congruent melting points of the alloys of Al with the transition metals. They assumed that in these alloys higher cohension was the result of increasing ionicity in the bond and suggested a charge transfer to the transition metal which should be maximum for Co–Al and decrease on both sides. Figure 7 gives direct experimental support to this interpretation.

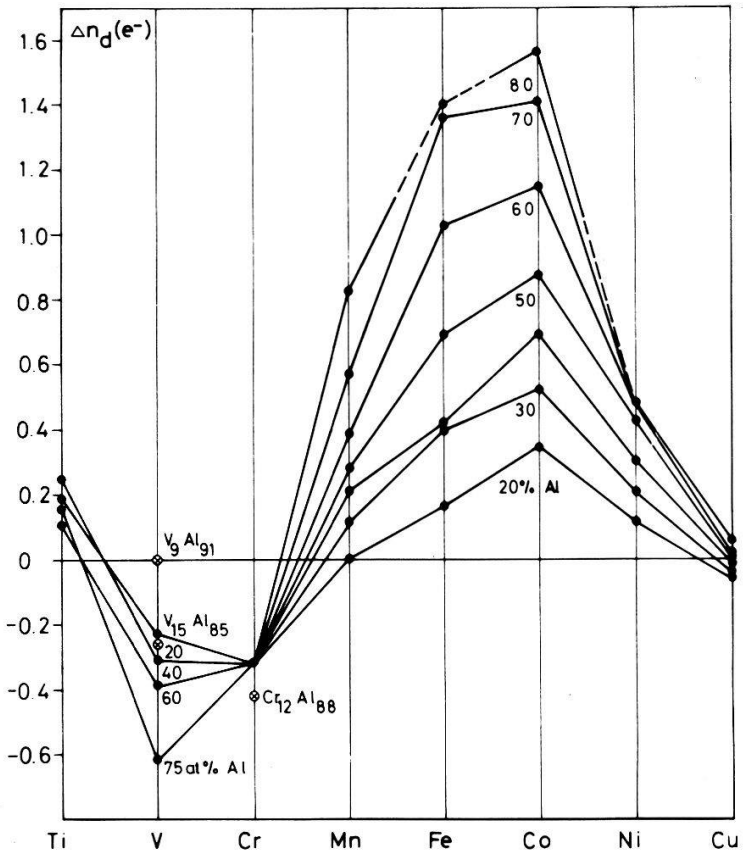

Figure 7
d charge transfers in the transition metal–aluminium alloys, traced over the transition metal for fixed aluminium content.

d) Although none of our alloys is dilute, the regular and systematic change of Δn_d as a function of concentration and of the element alloyed to Al suggest that, as far as Δn_d is concerned, the Al-richest alloys should not be qualitatively different from dilute solid solutions of transition metals in Al. The virtual bound states which form in these alloys should, according to Friedel [52], be unstable and be almost empty for elements like Ti and stable and full for elements like Ni; thus Δn_d should be negative in the first half of the series, positive in the second half. This is in agreement with the curves of Figure 7, except at the very beginning of the series where an empty *d* shell for Ti or V would give $\Delta n_d = -2$ to -4.

3.7. Change of the number of p electrons on Al atoms in the alloys Ti–, V–, Cr–, Mn–, Fe–, Co–, Ni–, Au–Al

Figures 8 and 9 give $R_K - 1$ (in %) and an estimate of the change by alloying, Δn_p, of the number of electrons of *p* symmetry in a WS sphere (see Section 1.3). These figures show the following facts: a) Δn_p is always positive and an order of magnitude smaller than the largest values of Δn_d. b) For the Al-rich alloys (down to

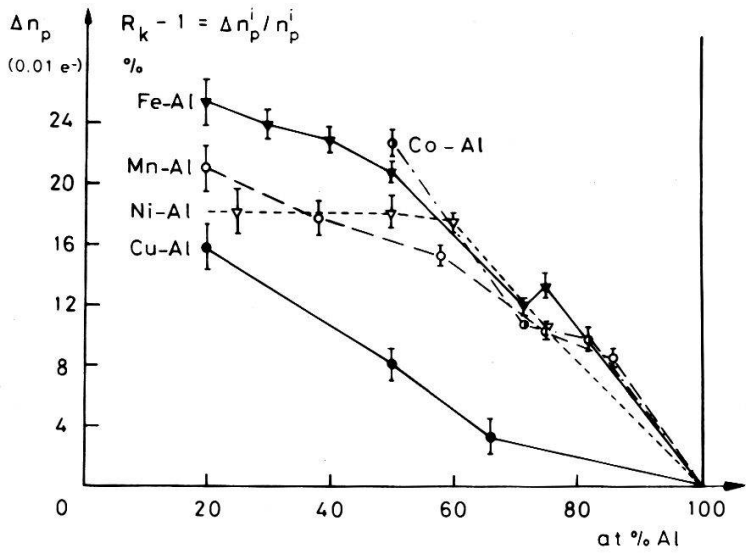

Figure 8
Ratio of integrated intensities, or charge transfer of p electrons, for the K_β band of aluminium for alloys of the right part of transition element series.

60% at. Al) the seven binary series Ti–Al to Ni–Al behave almost identically; n_p increases almost linearly with concentration, by about $0.004e^-$ per at.%. The change of n_p is much slower for Cu–Al. For Al concentrations lower than 60 at.%, the curves are again not very different for the various binary series but Δn_p shows a slower increase.

Over the whole transition metal series, there is no relation between Δn_d and Δn_p as exemplified by the case of Fe–Al and V–Al where Δn_p are similar, but Δn_d positive in the former and negative in the latter; there is no explanation for this at present. Various investigations and consistent interpretations, however, cover the alloys with elements of the second half of the transition metal series. For them Δn_p and Δn_d are positive. Thus a strong decrease in the number of s electrons is expected on Al sites. This has indeed been observed by Seitchik and Wamsley [53] in NMR studies of CoAl and NiAl, where the electron wave function (at the Fermi level) is found to have

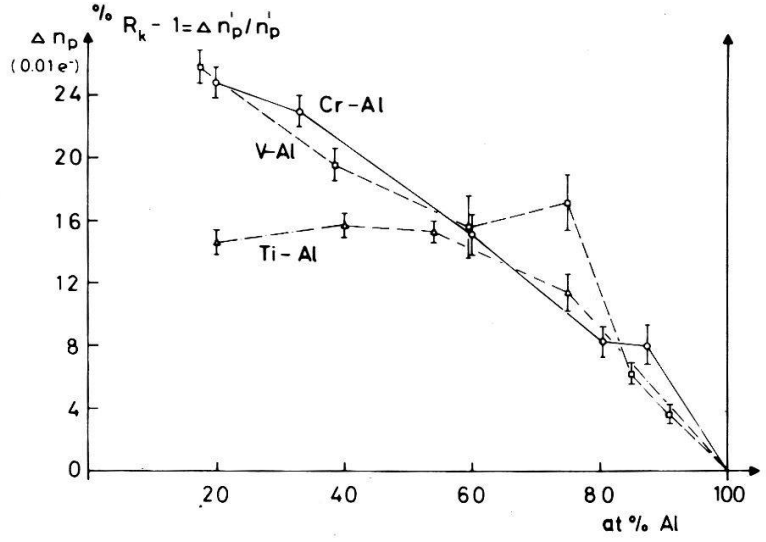

Figure 9
Ratio of integrated intensities, or charge transfer of p electrons, for the K_β band of aluminium for alloys of the left part of transition element series.

almost no s character on Al atoms. Vincze [54] notes further that the particular behaviour of Δn_p in the Ni–Al system (flat to about 60% at. Al) can well explain magnetic and Mössbauer data of Fe–Ni–Al alloys.

3.8. *Change of the* L_α $\{3d(4s) \rightarrow 2p^{3/2}\}$ *band width in the alloys V–, Cr–, Mn–, Fe–, Co–, Ni–, Cu–Al*

The width at half maximum of the L_α band is related (however perturbed by the broadening effects discussed in Section 1.1) to the energy interval occupied by the $3d$ electrons. For the alloys of interest here, this width has never been measured under weak reabsorption conditions. We therefore undertook these measurements, although the resolution of the microprobe spectrometer is not high for the elements at the end of the transition metal series. We were, in fact, mainly interested in the difference

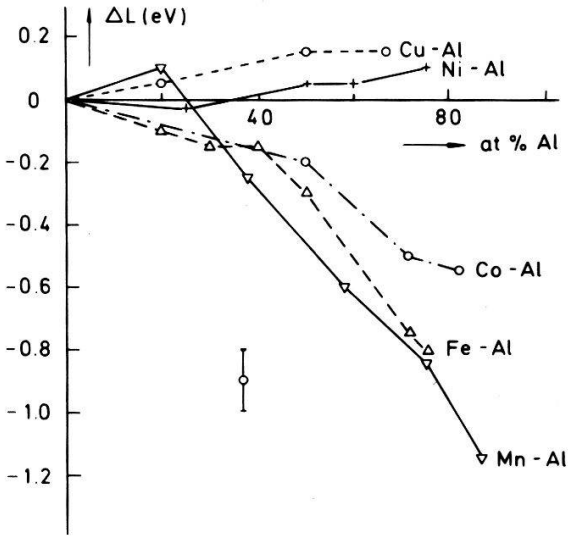

Figure 10
Change of the width of the L_α band by alloying transition metals (right part in series) with aluminium.

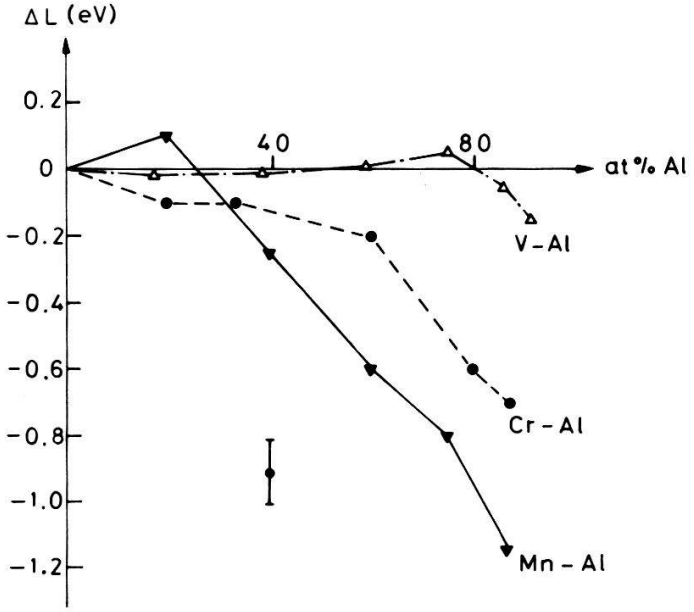

Figure 11
Change of the width of the L_α band alloying transition metals (left part in series) with aluminium.

$\Delta L = L$ (alloy)$-L$ (pure metal); for ΔL the resolving power is less important. A comparison of our L values with those obtained (for pure metals) with high resolution spectrometers has shown that the instrumental broadening should not affect the measured values of ΔL by more than 0.06 eV. For Ti–Al the width was not determined, because the lead stearate spectrometer crystal has a rather bad resolution.

Figures 10 and 11 give ΔL as a function of the Al concentration, c_{Al}, for the seven binary alloy series V–Al to Cu–Al. With the exception of Cu–Al, Ni–Al and V–Al, for which ΔL is almost equal to zero, ΔL decreases when going from the pure metal to the alloy. This is easily understood by noting that with increasing Al concentration the average distance between transition metal atoms increases, therefore the overlap of the $3d$ wave functions diminishes, which is known to decrease the band width [55]. Such a narrowing has been predicted by Rooke [10]. On the other hand no explanation can be offered for the fact that this narrowing is maximum at the centre of the period, i.e. for Mn alloys.

4. Results and Discussion: Cu–Ni Alloys

Cu–Ni alloys have been extensively studied. To account for the change of magnetization with concentration, Mott [55] assumed that the band structure is unaffected by alloying; Cu–Ni thus became the prototype of the rigid band model. Many experiments, however, were incompatible with this model and Coles [57], when explaining the anomalously high values of magnetic susceptibility and specific heat in the paramagnetic region, accepted the existence of d holes even in the Cu-rich alloys. This idea has been confirmed by a number of recent experimental results (many are cited in Ref. [58]) which, for the most part, were explained by the model of virtual bound states [58, 59]. The nickel d electrons (in Cu-rich alloys) are not part of the Cu d band, but are in virtual bound states, localized on Ni atoms, and whose energy lies approximately between the top of the Cu d band and the Fermi level. These bound states, which can accommodate 10 electrons, are only partially filled; there are thus d holes localized on Ni atoms. This model has also been used to explain photoemission results (Seib and Spicer [58], Myers et al. [60]).

The rigid band model is also in contradiction with measurements made on Ni-rich alloys. Lang and Ehrenreich [61] have shown that pressure dependence of the Curie temperature, with varying concentration, is of the opposite sense, as the rigid band model predicts. These authors then made a similar calculation, assuming that there were d holes only on Ni atoms and that their number was independent of Cu concentration; agreement with experiment was much better. In this so-called 'minimum polarity model' the electronic configuration of each type of atom ($\approx 3d^{9.5}4s^{0.5}$ and $3d^{10}4s^{1}$ for Ni and Cu respectively) is identical in the alloy and the pure metal; there is no charge transfer, and each atomic site is neutral. On the other hand, in the rigid band model a charge transfer is admitted from the Cu atom to the Ni atom, and bonding is partly ionic.

Integrated X-ray intensity measurements can, under the same conditions and with the same assumptions as for the transition metal–aluminium alloys, answer these questions. The results are shown in Figure 12. In the rigid band model, Δn_d would increase linearly up to 0.5 electrons/atom at 50 at.% of Cu and then remain constant. For the minimum polarity model, Δn_d does not change at all by alloying. For a resonant bound state, whose occupation is different from 10, again a charge transfer should appear. Myers et al. [60] described, for example, the d electrons on nickel in Cu-rich

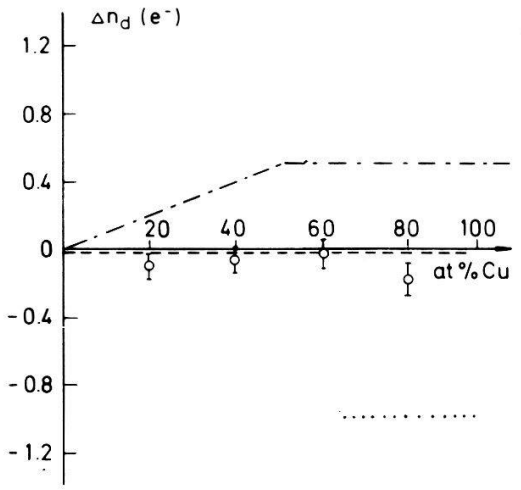

Figure 12
Measured d charge transfers in the Ni–Cu system compared with a behaviour consistent with the rigid band model (dashed, upper curve), the minimum polarity model (no charge transfer on the Ni atom) and a resonant bound state containing 8.5 electrons (dotted).

alloys by a narrow (1 eV width) resonant bound state containing 8.5 electrons. The results of Figure 12 give Δn_d with equation (11) and taking $n_d = 9.5$ for nickel. Clearly only the minimum polarity model is consistent with the findings.

5. Conclusions

We have shown the possibility of measuring, directly and quantitatively, the variation of the number of electrons in d- and p-like states upon alloying. This quantity is obtained from integrated X-ray emission intensities, using transitions from the band and an inner level which serves as internal reference. Such ratios, determined for the alloy and the pure metal, give the relative changes of the number of electrons (of a given orbital symmetry) inside the volume of the ion contributing to the emission. Experimental evidence showed further that these relative changes apply equally to band states. The method has been used to measure the changes of the number of d states in transition metal–aluminium alloys and Cu–Ni and of the number of p states in the Al atoms in the same alloys.

This study has somewhat deviated from its original purpose (determination of charge transfer) since we have measured changes of local and partial (that is of given orbital symmetry) charges. However, for the transition metals of the first series, and specially for those of the second half of the series, the two problems are similar, n_d being much larger than $n_{s,p}$. Moreover, the change of n_d by alloying is in fact even more interesting than that of the total number of electrons.

From a more technical point of view, the integrated intensities are of special value because they are the only X-ray spectroscopic quantities which are not affected by the broad inner level and Auger broadening. Finally we must note that the results presented should not be considered as definitive. A fundamental improvement would result if the measurements were made at excitation voltages below the L_2 level. This would eliminate the problems of reabsorption, of high-energy satellites, and of the L_α, L_β separation, and thus place the results on a firmer base.

Acknowledgments

The authors wish to acknowledge the support by the Swiss National Science Foundation. They thank F. Acker for the preparation of the Cu–Ni alloys, J. M. Suter and D. Robin for help in computing work, and Dr. N. Rivier for stimulating discussions. The authors owe a special debt of gratitude to G. Bürri, who has patiently and skilfully contributed to a difficult experimentation.

REFERENCES

[1] P. J. Black and W. H. Taylor, Rev. Mod Phys. *30*, 55 (1958); in *The Physics of Metals—1. Electrons* (Cambridge University Press 1969), p. 317.
[2] The influence of the chemical bond on integrated intensities of the X-ray emission band is first mentioned by Shubaev: A. T. Shubaev, Bull. Acad. Sci. USSR, Phys. Ser. *25*, 996 (1961).
[3] Preliminary reports: S. Steinemann and A. Wenger, Helv. Phys. Acta *41*, 129 (1968); A. Wenger, G. Bürri and S. Steinemann, Solid State Comm. *9*, 1125 (1971); A. Wenger, G. Bürri and S. Steinemann, Phys. Letters *3*, 195 (1971).
[4] H. A. Bethe and E. E. Salpeter, *Quantum Mechanics of One and Two Electron Atoms*, Chap IVa (Springer Verlag, Berlin—Göttingen 1957).
[5] D. A. Goodings and R. Harris, J. Phys. C, Ser. 2, 1808 (1969).
[6] C. Bonnelle, Ann. Physique *1*, 439 (1966).
[7] H. W. B. Skinner, Phil. Trans. Roy. Soc. *239*, 95 (1940).
[8] I. Ya. Nikifnov, Phys. Met. Metall. *11*, 100 (1961).
[9] M. A. Blokhin and V. P. Sachenko, Izv. Akad, Nauk SSSR, ser. fiz. *24*, 397 (1960).
[10] G. A. Rooke, in *Soft X-Ray Band and the Electronic Structure of Metals and Materials*, edited by D. J. Fabian (Academic Press, London and New York 1968), p. 185.
[11] J. H. Wood, Phys. Rev. *117*, 714 (1960).
[12] J. R. Cuthill, A. J. McAlister, M. L. Williams and M. E. Watson, Phys. Rev. *164*, 1006 (1967).
[13] J. C. Slater, *Quantum Theory of Atomic Structure*, Vol 1 (McGraw-Hill 1960), p. 230.
[14] F. Herman and S. Skillmann, *Atomic Structure Calculations* (Prentice-Hall, Inc., Englewood Cliffs, N. Jersey 1963).
[15] E. C. Snow and J. T. Waber, Acta Metallurgica *17*, 623 (1969).
[16] N. F. Mott, Adv. in Phys. *13*, 325 (1964).
[17] W. Hume-Rothery and B. R. Coles, Adv. in Phys. *3*, 149 (1954).
[18] J. Felsteiner, R. Fox and S. Kahane, Solid State Comm. *9*, 457 (1971).
[19] R. J. Weiss, Phys. Rev. Lett. *24*, 883 (1970).
[20] K. F. Berggren, Phys. Rev. *B6*, 2156 (1972).
[21] R. J. Liefeld, in *Soft X-Ray Band and the Electronic Structure of Metals and Materials*, edited by D. J. Fabian (Academic Press, London and New York 1968), p. 133.
[22] In a recent article, B. Dev and H. Brinkman, Physica *57*, 616 (1972), in order to obtain the 'undisturbed' shape of the Cu L_α band, have recorded this spectra at voltages below the L_2 level, they get a width of half maximum 1 eV smaller than that obtained by Liefeld [21] at the same voltage. The massive sample was introduced into the spectrometer (10^{-8} torr) and then measured at room temperature, apparently without *in situ* cleaning of the surface. Under these conditions, they have in fact measured the natural oxide layer (which is of the order 10–30 Å). This is confirmed by the comparison of their width with that obtained by Bonnelle [6] for copper oxide, 2.0 ± 0.1 eV. By contrast Liefeld worked at high temperature (and at 10^{-9} torr) and could thus have a clean surface. But with alloys it is often not possible to work at high temperature (some of the Al alloys melt under 600°C).
[23] R. L. Barinski and W. I. Nefedov, *Röntgenspektroskopische Bestimmung der Atomladung in Molekulen, Leipzig 1969* (Akademische Verlagsgesellschaft), p. 215.
[24] R. Manne, J. Chem. Physics *46*, 4645 (1967).
[25] W. G. Sirianov, W. J. Minin, S. A. Nemnonov and M. F. Sorukina, Fiz. Met. Metalloved *31*, 335 (1971).
[26] K. Siegbahn, C. Nordling, A. Fahlman, R. Nordberg, J. Hamrin, K. Hedman, G. Johansson, T. Bergmark, S. E. Karlsson, I. Lindgren and B. Lindberg, Annales de Physique *3*, 281 (1968).

[27] W. KENNE and A. TRAUTWEIN, Metall. *25*, 27 (1971).
[28] G. FOEX and J. WUCHER, C. R. Acad. Sci. *238*, 1283 (1954).
[29] J. WUCHER and G. FOEX, J. Phys. Rad. *17*, 454 (1956).
[30] M. HÖHL, Z. Metallk. *51*, 85 (1960).
[31] W. KÖSTER, E. WACHTEL and K. GRUBE, Z. Metallk. *54*, 393 (1963).
[32] W. W. KOPP and E. WACHTEL, Z. Metallk. *60*, 771 (1969).
[33] V. YA. NAGORNYI and V. V. NEMOSHKALENKO, Sov. Phys. Dokl. *11*, 161 (1966).
[34] L. D. FINKEL'SHTEYN and S. A. NEMNONOV, Phys. Met. Metall. *26*, 102 (1968).
[35] A. P. LUKIRSKII and I. A. BRYTOV, Trans. Bull. Acad. Sci. USSR, Phys. Ser. *28*, 749 (1965).
[36] A. WENGER, Transferts de charge dans les alliages des métaux de la première série de transition avec l'aluminium et dans les alliages cuivre-nickel mesurés par spectroscopie de rayons-X, Thèse Université Lausanne, 1972.
[37] V. F. VOLKOV and L. A. ROSSOKA, Phys. Met. Metall. *25*, 185 (1968).
[38] L. RUDSTRÖM, Arkiv för Fysik *12*, 287 (1957).
[39] S. A. NEMNONOV and L. D. FINKEL'SHTEIN, Bull. Acad. Sci. USSR, Phys. Ser. (USA) *25*, 1015 (1961).
[40] G. V. RAYNOR, Prog. Metal Phys. *1*, 1 (1949).
[41] L. PAULING, Acta Cryst. *4*, 138 (1951).
[42] M. A. TAYLOR, Proc. Phys. Soc. *78*, 1244 (1961).
[43] M. HÖHL, Annalen der Physik *19*, 15 (1967).
[44] S. R. BUTLER, J. E. HANLON and R. J. WASILEWSKI, J. Phys. Chem. Solids *30*, 1929 (1969).
[45] G. W. WEST, Phil. Mag. *15*, 855 (1967).
[46] F. R. DEBOER, G. J. SCHINKEL, J. BIESTERBAS and S. PROOST, J. Appl. Phys. *40*, 1049 (1969).
[47] D. M. EDWARDS, Phys. Lett. *33A*, 183 (1970).
[48] T. M. SRINIVASAN and H. CLAUS, J. Phys. Chem. Solids *28*, 711 (1967).
[49] P. J. BROWN, Acta Cryst. *12*, 995 (1959).
[50] A. D. CAPLIN, G. GRÜNER and J. B. DUNLOP, Phys. Rev. Lett. *30*, 1138 (1973).
[51] A. E. RAY and J. F. SMITH, Acta Cryst. *13*, 876 (1960).
[52] J. FRIEDEL, Nuovo Cim. Suppl. *8*, 287 (1958).
[53] J. A. SEITCHIK and R. H. WAMSLEY, Phys. Rev. *137*, A143 (1965).
[54] I. VINCZE, Phys. Rev. B *7*, 54 (1973).
[55] N. F. MOTT and H. JONES, *The Theory of the Properties of Metals and Alloys*, 1936.
[56] N. F. MOTT, Phil. Mag. *22*, 287 (1936).
[57] B. R. COLES, Proc. Phys. Soc. *B65*, 221 (1952).
[58] D. H. SEIB and W. E. SPICER, Phys. Rev. B, *2*, 1676 (1970).
[59] P. W. ANDERSON, Phys. Rev. *24*, 41 (1961).
[60] H. P. MYERS, C. NORRIS and L. WALLDEN, Solid State Comm. *7*, 1539 (1969).
[61] N. D. LANG and H. EHRENREICH, Phys. Rev. *168*, 605 (1968).